Experimental study of the effective nucleon-nucleon interaction using the ^{21}F$(d,p)^{22}$F reaction

J. Chen,[1,*] C. R. Hoffman,[1] T. Ahn,[2] K. Auranen,[1] M. L. Avila,[1] B. B. Back,[1] D. W. Bardayan,[2] D. Blankstein,[2] P. Copp,[3,1] D. Gorelov,[4,1] B. P. Kay,[1] S. A. Kuvin,[5,1] J. P. Lai,[2] D. G. McNeel,[5,1] P. D. O'Malley,[2] A. M. Rogers,[3] D. Santiago-Gonzalez,[6,1] J. P. Schiffer,[1] J. Sethi,[7,1] R. Talwar,[1] and J. R. Winkelbauer[8]

[1]*Physics Division, Argonne National Laboratory, Argonne, Illinois 60439, USA*
[2]*Department of Physics, University of Notre Dame, Notre Dame, Indiana 46556-5670, USA*
[3]*Department of Physics and Applied Physics, University of Massachusetts Lowell, Lowell, Massachusetts 01854, USA*
[4]*University of Manitoba, Department of Physics and Astronomy, Allen Building, Winnipeg, Manitoba R3T 2N2, Canada*
[5]*Department of Physics, University of Connecticut, Storrs, Connecticut 06269, USA*
[6]*Department of Physics and Astronomy, Louisiana State University, Baton Rouge, Louisiana 70803, USA*
[7]*Department of Chemistry and Biochemistry, University of Maryland, College Park, Maryland 20742, USA*
[8]*Los Alamos National Laboratory, Los Alamos, New Mexico 87545, USA*

(Received 29 May 2018; published 25 July 2018)

The single-neutron configurations of several low-lying states in ^{22}F have been determined from neutron-adding cross sections of a (d,p) reaction using a ^{21}F radioactive beam in inverse kinematics. Final states in ^{22}F consisting of a proton in the $\pi 0d_{5/2}$ orbital coupled to a neutron in either the $\nu 0d_{5/2}$, $\nu 1s_{1/2}$, or $\nu 0d_{3/2}$ orbitals were observed up to an excitation energy of ∼5 MeV. Spectroscopic factors and strengths were determined from the angular distribution of the cross sections using a distorted wave Born approximation method. The distribution of the $\nu 0d_{5/2}$ and $\nu 1s_{1/2}$ strength was well described by all USD effective shell model interactions, while only the more recent USDA/USDB interactions showed a marked improvement in describing the observed $\nu 0d_{3/2}$ strength. Diagonal two-body matrix elements of the $(0d_{5/2})^2_{J=0-5}$ effective nucleon-nucleon interaction were extracted from the data and compared with previous determinations of the same matrix elements from particle-particle and hole-hole spectra, as well as the calculated results of the USDA interactions. No significant discrepancies were observed. Inspection of the monopole energies showed that an improved agreement between the different empirical matrix elements is found if a mass dependence is included.

DOI: 10.1103/PhysRevC.98.014325

I. INTRODUCTION

The shell model of Mayer and Jensen [1,2] has been enormously successful, assuming that nucleons move in an average potential and that the details of the nuclear structure depend on an effective residual interaction whose matrix elements are determined empirically. Early in the history of the shell model [3,4] fits with such matrix elements gave a good account of many nuclear structure properties. Such calculations have been refined in recent years and much of the data on nuclear structure are parametrized by them [5,6].

Odd-odd nuclei around doubly closed shells have been extensively used to investigate effective nucleon-nucleon (NN) interactions in nuclei. In particular, information pertaining to the multiplets of levels formed by the coupling of the valence proton and neutron orbitals, $\pi n\ell_j$ and $\nu n\ell_j$, has allowed for the extraction of two-body matrix elements (TBMEs) in nuclei across the nuclear chart. Global surveys of the empirical diagonal TBMEs from transfer data indicated some common properties of the residual interaction and that the diagonal matrix elements of the interaction from the $0p$ shell to ^{208}Pb could be described reasonably well by a single empirical two-body potential acting on harmonic-oscillator wave functions [7]. With the current availability of radioactive beams, systematic investigations based on TBMEs continue to remain key quantitative tools in describing the effective NN interaction with respect to shifts away from stability, and consequently binding energy, which may imply changes from the simple assumptions of oscillator wave functions.

The even-A fluorine isotopes ($Z = 9$) have played, and will continue to play, an important role in explorations of TBMEs due to the large number of doubly magic oxygen isotopes ($Z = 8$). For each odd-odd F isotope residing near one of these doubly magic nuclei, at neutron numbers $N = 8$, 14, 16, and possibly 20 [8], the single proton in a $0d_{5/2}$ orbital will be coupled to a neutron (or neutron hole) residing in one of the various sd orbitals above $N = 8$ ($\nu 0d_{5/2}$, $\nu 1s_{1/2}$, and $\nu 0d_{3/2}$). Therefore, across a single isotopic chain, it allows for the extraction of empirical TBMEs over a large range of proton-to-neutron ratios and binding energies.

Recent work along these lines has taken place for the multiplet of levels occurring from a proton in the $0d_{5/2}$ orbital coupled to a neutron in the $0d_{3/2}$ orbital in ^{26}F, ^{28}Na, and ^{30}Al [9–11]. There, the relevant TBMEs, labeled as $E_J^{(p-p)}(0d_{5/2}0d_{3/2})$, were shown not to be described well by effective sd-shell interactions, such as the USDA interaction [12], possibly related to the binding energies of the orbitals.

*jie.chen@anl.gov

In particular, ^{26}F levels were systematically overbound by ∼30–40 % of the total interaction strength (∼300 keV). An analogous situation was also observed between analog levels in the proton-unbound $1s_{1/2}$ state in ^{16}F relative to the bound neutron state in ^{16}N [13].

Diagonal TBMEs resulting from a proton and a neutron both residing in a $0d_{5/2}$ orbital, $E_J^{(p-p)}(0d_{5/2}{}^2)$, have been deduced from ^{18}F and ^{18}O particle-particle spectra aiding in the foundation of an effective interaction encompassing the sd shell [7]. The $E_J^{(p-p)}(0d_{5/2}{}^2)$ TBMEs from ^{18}F-^{18}O can also be compared to equivalent $E_J^{(p-p)}(0d_{5/2}{}^2)$ extracted from ^{26}Al and ^{26}Mg hole-hole spectra. Reasonable agreement can be found between these two cases on the order of a few hundred keV, in particular when an A-dependence of the TBMEs is considered, even with concerns surrounding the robustness of ^{28}Si to serve as a doubly magic core [7].

The one-neutron transfer reaction is a powerful tool to study the single-particle structure of nuclei [14–17]. In the present work, one-neutron adding (d,p) reaction on ^{21}F is used to explore the single-particle structure of the low-lying states in ^{22}F. A summary of previously identified levels in ^{22}F, along with their possible spin-parity assignments, are shown in Fig. 2 [18]. ^{22}F has been investigated through charge-changing reactions on ^{22}Ne including (n,p) [19], $(t,{}^3\mathrm{He})$ [20,21], and $({}^7\mathrm{Li},{}^7\mathrm{Be})$ [22]. Relevant to the present work are the states with excitation energies of $E_x = 0.071, 0.709, 1.414$, and 1.63 MeV which have been assigned as $J^\pi = 3^+$, $(2,3^+)$, 5^+, and 3^+, respectively, as well as a number of levels with ill-defined spins between $E_x \approx 2.5$–5.5 MeV. A spin-parity of 4^+ was assigned to the ground state based on its allowed β-decay branches to known states in ^{22}Ne [23]. Similarly, spin-parity assignments of 1^+ were made to the states at 1.63 and 2.572 MeV in ^{22}F based on the β-decay study of ground state of ^{22}O [24]. An electromagnetic transition study using the fusion-evaporation reaction $^9\mathrm{Be}(^{14}\mathrm{C},p)$ and γ-ray detection [25] found a doublet of states at 1.628 and 1.633 MeV which clarified the apparent controversial results of the previous measurements [20,21,24]. A number of excited levels up to $E_x \approx 3.6$ MeV were also observed and a number of suggested spin assignments were made, including $J^\pi = 2^+$ for the 2.007 MeV state.

The ground state of ^{21}F is known to have $J^\pi = 5/2^+$ resulting from a single unpaired proton occupying the $\pi 0d_{5/2}$ orbital coupled to four neutrons predominantly coupled to $J = 0$ and partially filling the $\nu 0d_{5/2}$ orbital outside of an $N = Z = 8$ core [26]. The addition of one neutron onto the ^{21}F ground state could result in occupancy of either the $0d_{5/2}$ ($\ell = 2$), $1s_{1/2}$ ($\ell = 0$), or $0d_{3/2}$ ($\ell = 2$) orbitals and final-state J^π values of 0^+–5^+, 2^+–3^+ or 1^+–4^+, respectively. For sd-shell nuclei with $Z < 10$, most of the $\ell = 2$ strength belonging to the neutron $0d_{5/2}$ orbital lies below an excitation energy of ∼2 MeV while the $0d_{3/2}$ strength has been observed at much higher energies ($E_x \gtrsim 4$–5 MeV) [17,27–29]. Similarly, the bulk of the $\ell = 0$ neutron $1s_{1/2}$ strength typically lies below $E_x \approx 2$–3 MeV. This information gives a general guide as to where the multiplets of expected states should lie in ^{22}F.

Extraction of the TBMEs from the single-neutron strengths in ^{22}F relies on a robust doubly magic ^{22}O core. Evidence for a large neutron subshell closure at $N = 14$ can be found in trends in the one-neutron separation energies [30], relative transition strengths and energies of the yrast states compared to neighboring even-even nuclei [31], and information with respect to the $\nu 0d_{5/2}$-$\nu 1s_{1/2}$ single-particle energy gap [32]. In terms of the proton shell closure, there is a large amount of data supporting a robust proton $\pi 0p_{1/2}$-$\pi 1s_{1/2}$ $Z = 8$ shell gap in the neutron-rich oxygen isotopes [30,31]. In addition, data from the $^{22}\mathrm{Ne}(d,{}^3\mathrm{He})^{21}$F reaction showed that the ^{21}F $5/2^+$ ground state carried >70% of the proton $0d_{5/2}$ strength [33], which is consistent with a closed $Z = 8$ proton shell and restricts the valance proton to the $\pi 0d_{5/2}$ orbital in ^{22}F for states populated strongly in the $^{21}\mathrm{F}(d,p)$ reaction.

In the present work, the neutron single-particle structure in ^{22}F ($Z = 9$, $N = 13$) has been investigated using the $^{21}\mathrm{F}(d,p)^{22}$F reaction. The spectroscopic strength distribution in ^{22}F was extracted from the transfer cross sections through a distorted wave Born approximation (DWBA) analysis. Diagonal TBMEs of the type $E_J^{(p-p)}(0d_{5/2}{}^2)$ were deduced from the $0d_{5/2}$ proton and $0d_{5/2}$ neutron particle-hole centroids. Comparisons to previous determinations of the $E_J^{(p-p)}(0d_{5/2}{}^2)$ extracted from only particle-particle and hole-hole data are made. A number of conclusions concerning the weakening of the empirically derived effective NN interaction relative to shell-model calculations with sd-shell effective interactions and the possible A-dependence of effective TBMEs are also obtained. Additionally, a discussion of the reproduction of the strength-distribution by shell-model calculations using the USD, USDA, and USDB sd-shell confined interactions [5,12] is presented.

II. EXPERIMENT

The $^{21}\mathrm{F}(d,p)^{22}$F reaction was carried out at the Argonne National Laboratory ATLAS In-Flight Facility [34]. The 10 MeV/u radioactive ^{21}F beam was produced via proton removal from a 250 pnA $^{22}\mathrm{Ne}^{10+}$ primary beam at 11 MeV/u on a 5 mg/cm^2 Be target. The ^{21}F beam intensity was approximately 2–4 × 10^4 particles per second (pps) and had a purity ranging from 10%–80%, the primary contaminant being $^{22}\mathrm{Ne}^{8+}$. Data from the $^{22}\mathrm{Ne}(d,p)^{23}$Ne reaction at 11 MeV/u were used for energy calibrations and as a check in the analysis procedure.

The measurement was carried out using the HELIcal Orbit Spectrometer (HELIOS) [35,36] with a magnetic field strength of 2.5 T and the experimental setup resembled that shown in Fig. 2 of Ref. [17]. Deuterated polyethylene (CD_2) targets of thickness 200 μg/cm^2 were used, and they were placed near the center of the magnet ($Z \approx 0$ cm). The position-sensitive Si detector (PSD) array covered a range of $-56 < Z < -21$ cm upstream from the target. A Si detector to monitor deuterons scattered from the target, a Si telescope to identify recoiling nuclei (nominally 80 μm and 500 μm thick), and an on-axis zero-degree Si detector telescope to monitor the rate of the beam (nominally 80 μm and 500 μm thick), were located at $Z = 12$, 108, and 113 cm, respectively, downstream from the target. A perforated Ta plate was used in front of the zero-degree Si telescope to attenuate the beam rate by a factor of ∼1000 during the measurement. The energy response of the

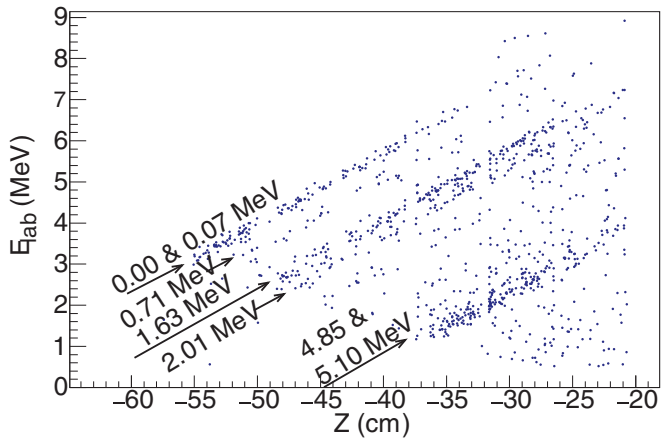

FIG. 1. Measured proton energies ($E_{\rm lab}$) as a function of the distance from the target (Z) for the ^{21}F$(d,p)^{22}$F reaction in inverse kinematics at 10 MeV/u with a magnetic field strength of 2.5 T. The proton data shown required a coincidence with ^{22}F in the recoil detector telescope. Final states identified in ^{22}F, appearing as tilted parallel lines, are indicated by arrows and are labeled by their corresponding excitation energy.

PSDs were calibrated using the well-known Q values of the ^{22}Ne$(d,p)^{23}$Ne reaction to the ground and low-lying excited states [37].

Reaction channels other than ^{21}F$(d,p)^{22}$F were removed by requiring a timing coincidence within 150 ns between a proton detected in a PSD and a ^{22}F recoil—identified via the ΔE-E signals of the Si recoil telescope. The timing coincidence also removed the bulk of the uncorrelated background and made it negligible in the analysis. The energies of protons selected with this method ($E_{\rm lab}$) are plotted versus their corresponding longitudinal distance from the target (Z) in Fig. 1. A ^{22}F excitation energy spectrum was deduced from a projection of the tilted parallel lines found in Fig. 1, and is shown in Fig. 2. The excitation energies, E^*, of levels in ^{22}F resulting from a multigaussian fit to the excitation spectrum using a fixed FWHM and free parameters for the centroids and amplitudes, are presented in Table I. The excitation energy spectrum has a resolution of approximately 200 keV FWHM due to properties of the in-flight radioactive beam, as well as the energy losses and the energy/angle straggling of the charged particles in the target.

The measured angular distributions for final states observed in ^{22}F are shown with their statistical uncertainties by the black data points in Fig. 3. Each single PSD, of which there were six longitudinally and four azimuthally [36], was either considered as a single center-of-mass angular bin, or separated into two bins where the statistics allowed. Relative cross sections were determined from the measured proton yields in each of the defined angular bins. The center-of-mass angle for a bin, $\theta_{\rm c.m.}$, was determined from the reaction kinematics and the properties of HELIOS (see Eq. (3) in Ref. [17]). Uncertainties on $\theta_{\rm c.m.}$ are less than 1°. The center-of-mass solid-angle covered for a single PSD was approximately 30 msr for the ^{21}F$(d,p)^{22}$F reaction and the present setup. The minimum detection angle of the recoil detector, and the proton-recoil coincident requirement, limited the angular distribution to $\theta_{\rm c.m.} > 10°$.

Deuterons produced from the elastic scattering of ^{21}F on the deuterium in the CD_2 targets were selected by a required coincidence between deuterons found in the monitor Si detector and ^{21}F recoils identified in the Si recoil detector telescope, as in Refs. [38,39]. The deuterons were measured at an energy of ∼2 MeV and at an angle of $\theta_{\rm c.m.} \approx 20°$, where the scattering cross sections are ≈30% larger than Rutherford cross sections. The number of the ^{21}F beam particles hitting the target was obtained by dividing the number of the scattered deuterons by calculated cross sections using the optical model potential, and included the acceptance of the experimental setup. Absolute cross sections were obtained combing this information with the target thickness, PSD solid angle, and observed counts. Different optical model parameter sets [40–44] were explored in the calculations of the scattering cross sections. The resulting cross sections varied with an rms of ∼17%. Due to the limited statistics in the monitor detector, and the varying results of the calculations, the overall uncertainty on absolute cross sections is ≈30%. This uncertainty does not impact the discussions to follow as they are based on the relative yields.

III. RESULTS

The ^{22}F excitation energy spectrum deduced in the present work is shown in Fig. 2 together with states examined in previous works (upper panel) [18]. The 4^+ ground state and the 3^+ 0.072-MeV doublet could not be separated, and no significant strength was observed at 300 keV, the location of a state observed in a charge-exchange reaction [20]. Excited states at 0.71(2), 1.63(1), 2.01(1) MeV were resolved in the spectrum, and they correspond to previously observed levels at $E^* = 0.709$, 1.628/1.633, and 2.007 MeV having $J^\pi = 2^+$, $1^+/3^+$ and 2^+, respectively. As discussed below, no individual strength was observed belonging to the $J^\pi = 1^+$, 1.628 MeV state, which will be discussed in Sec. IV. Hence, it is assumed that the observed 1.63-MeV peak is dominated by the 1.633-MeV 3^+ level. The small shoulder that manifests itself at the lower energy side of the 1.63-MeV peak, however, could be a signature of the previously observed $J^\pi = 5^+$ state at 1.414 MeV. Only an upper limit on the yield was determined for this state.

A large amount of yield is found at ∼5 MeV in the spectrum of Fig. 2, a region where no definitive levels had been previously reported. The width of the ∼5 MeV peak (∼0.4 MeV FWHM) is wider than the expected resolution (≈200 keV FHWM), indicating the presence of more than one single state in this region. A fit to the data around ∼5 MeV using a double-Gaussian function, with free parameters for the amplitudes and centroids but with widths fixed to the known experimental resolution, returned two levels at $E^* = 4.85(5)$ and 5.10(3) MeV. Only these two states are assumed for the discussions below, although additional levels of varying strength may also be present.

Some single-particle strength is also found in the range of $2.2 < E^* < 4.6$ MeV. Due to the limited statistics, angular distributions for these states were not possible. However, upper limits on strengths for a few of the features were extracted

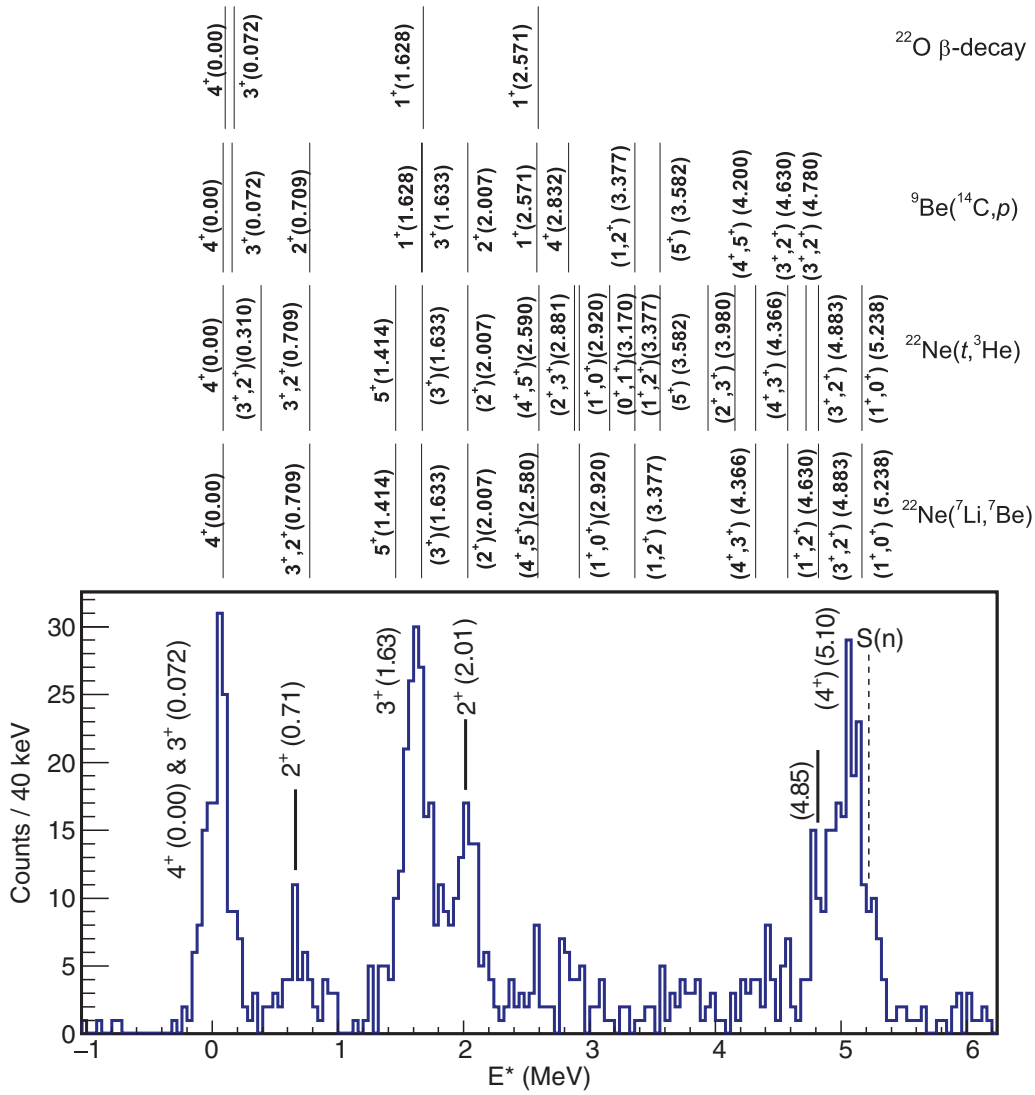

FIG. 2. The excitation-energy spectrum of ^{22}F as determined from the ^{21}F(d,p) reaction from the same data set as presented in Fig. 1. States clearly identified in the present work are labeled with their corresponding spin assignments. The states that have been observed in previous measurements are shown in the upper panel for comparison [18].

from integrated yields as detailed below (Table I). Of the large number of levels populated strongly in this region by other types of reactions (Fig. 2), none appear to be of dominant single-neutron character. Additionally, as many of the known levels have suggested J values of 0 or 1, their expected yields would have been small to begin with.

Assignments of orbital angular momentum to the neutron transfer, ℓ, and spectroscopic factors, S (for this reaction the isospin coefficient $C^2 = 1$), between the ^{21}F ground state and final states in ^{22}F were extracted from the measured angular distributions through a DWBA analysis utilizing the program PTOLEMY [45]. The optical-model parameter sets of An *et al.* [44] and Koning-Delaroche *et al.* [42] were used to define the potentials of the entrance and outgoing channels, respectively. The Argonne V_{18} [46] potential was used to define the deuteron bound-state wave function and a Woods-Saxon potential with central potential well parameters of $r_0 = 1.25$ fm and $a = 0.65$ fm, and with spin-orbit parameters of $V_{so} = 6.0$ MeV, $r_{so} = 1.1$ fm, and $a_{so} = 0.65$ fm, was used to define the final bound-state wave function of the neutron. The depth of the Woods-Saxon potential well was adjusted to reproduce the correct binding energy of each of the final states in ^{22}F.

The calculated angular distributions from DWBA were normalized to the available data using a standard χ^2 minimization method, the results of which are shown in Fig. 3. The extracted spectroscopic factors, and their corresponding strengths,

$$GS = \frac{2J_f + 1}{2J_i + 1} S, \tag{1}$$

where $J_i = 5/2$ and J_f is the spin of the final state in ^{22}F, are listed in Table I. The uncertainties in the relative S arise from statistics, the fitting procedure, and variations in the DWBA analysis. In total they sum to ≈10% for the $\ell = 2$ strength and ≈17% for $\ell = 0$ strength. For the weaker states observed in Fig. 2 in which angular distributions were not possible, upper limits on their strength were determined from a ratio

TABLE I. Spectroscopic factors (S) and spectroscopic strengths (GS) for states in ^{22}F measured by the ^{21}F$(d,p)^{22}$F reaction at 10 MeV/u. Relative uncertainties on S and GS are shown in parenthesis. Details on the uncertainties, $\ell = 2$ and $\ell = 0$ normalization factors, and assignments of J^π and nlj is found in the text.

E*(MeV)	$\ell(\hbar)$	J^π	nlj	S	GS
0.00 & 0.071[a]	2	4^+ & 3^+	$0d_{5/2}$	0.95(9)	1.48(11)
	0	3^+	$1s_{1/2}$	0.22(7)	0.27(8)
0.71(2)	2	2^+	$0d_{5/2}$	0.30(7)	0.24(6)
	0	2^+	$1s_{1/2}$	0.09(5)	0.07(5)
1.4(1)	2	5^+	$0d_{5/2}$[a]	<0.1[b]	<0.2
1.63(1)	0	3^+	$1s_{1/2}$	1.01(15)	1.18(18)
	2	3^+	$0d_{5/2}$	⩽0.05	⩽0.05
2.01(1)	0	2^+	$1s_{1/2}$	0.67(10)	0.56(9)
	2	2^+	$0d_{5/2}$	⩽0.05	⩽0.05
2.6(1)	2	1^+		<0.4[b]	<0.2
2.8(1)	2	(4^+)		<0.2[b]	<0.3
3.7(1)	2				<0.2[b]
4.4(1)	2				<0.3[b]
4.85(5)	2	$(1^+ - 4^+)$	$0d_{3/2}$	0.25(5)[c]	0.21(5)
5.10(3)	2	(4^+)	$0d_{3/2}$	0.98(8)[c]	1.47(11)

[a]Based on previous work [18].
[b]Limits obtained from integrated cross section assuming $\ell = 2$.
[c]Same normalization as $0d_{5/2}$ levels.

of measured-to-calculated integrated cross sections, assuming in all cases an $\ell = 2$ neutron transfer (Table I).

The angular distribution for the combined ground and 0.07 MeV levels, as well as the 0.71 MeV distribution, were best reproduced by composite $\ell = 0$ and 2 DWBA distributions (Fig. 3). These mixed distributions are consistent with the previous spin assignments for these levels of 4^+, 3^+, and 2^+, respectively [18]. Within ∼1.5−2.2 MeV excitation energy, the $\ell = 0$ strengths of the 1.63-MeV and 2.01-MeV states dominate the yields. Upper limits on the $\ell = 2$ strength were observed only at the few percent level (Table I). The dominance of $\ell = 0$ strength at $E^* = 1.63$ MeV is evidence for population of the 3^+ state over the 1^+ state, considering the latter is only reachable via $\ell = 2$ neutron transfer. The $\ell = 0$ distribution for the 2.01-MeV state is also consistent with its previous 2^+ assignment. Both levels observed around $E^* = 5$ MeV show pure $\ell = 2$ angular distributions as expected for levels at this excitation energy.

In the present measurement, the bulk of the $\nu 0d_{5/2}$ and $\nu 1s_{1/2}$ strength has been observed (further details supporting this are given in Sec. IV). Assuming that all the $d_{5/2}$ strength was below ∼2.1 MeV and all $d_{3/2}$ strength at energies higher than this, we obtain a normalization of S values according to the Macfarlane and French sum rules [45]. In a simple single-particle picture, both orbitals should have vacancies of 2, giving $\sum GS_{0d_{5/2}} = 2$ and $\sum GS_{1s_{1/2}} = 2$. All levels labeled in Table I by either $\nu 0d_{5/2}$ or $\nu 1s_{1/2}$, were included in their respective normalization sums. The final normalizations were 0.62 and 1.25 for the $\nu 0d_{5/2}$ and $\nu 1s_{1/2}$, respectively.

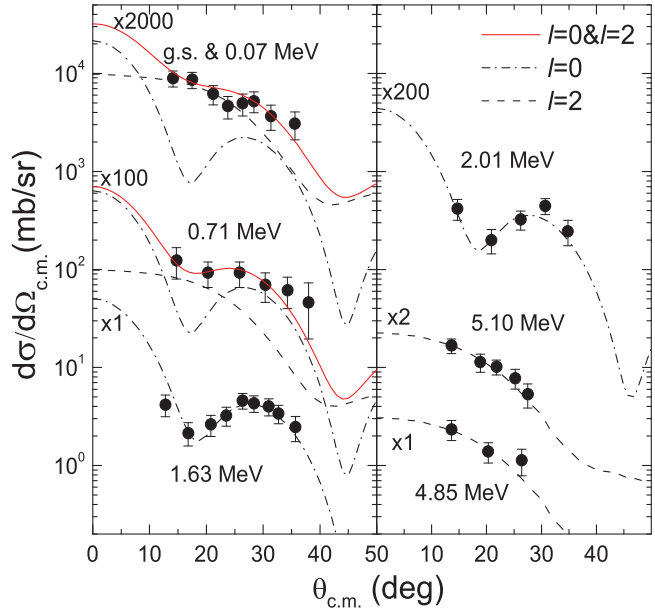

FIG. 3. Experimental (black points) and calculated (lines) cross sections as a function of the center-of-mass angle for various final states in the reaction ^{21}F$(d,p)^{22}$F at 10 MeV/u. Only statistical uncertainties are shown for the experimental data, and there is a systematic uncertainty of ∼30% on the absolute cross section scale. The dashed and dot-dashed curves are the calculated DWBA cross sections for $\ell = 2$ and $\ell = 0$ neutron transfer, respectively. The red solid curves are the resulting fits which incorporated mixed $\ell = 0$ and $\ell = 2$ angular distributions. Note the multiplication factors used for the ease of plotting.

The entirety of the procedures for the extraction and normalization of the spectroscopic factors was validated using the ^{22}Ne(d,p) data at 11 MeV/u taken with the same experimental setup. Use of the optical model parameters listed above in the DWBA analysis produced normalized spectroscopic factors and strengths consistent with those obtained in Ref. [47], for both $\ell = 0$ and $\ell = 2$ neutron transfer.

IV. DISCUSSION

In ^{22}F, the ground state and the two excited states at 0.071 and 0.71 MeV account for ∼85% of the observed $0d_{5/2}$ single-neutron strength (Table I). The dominant components of the $\ell = 0$ strength, the 1.63- and 2.01-MeV levels, account for ∼85% of the observed $0s_{1/2}$ single-neutron strength. The E^* of these two strengths are in-line with their expected single-particle energies, based on a simple single-neutron coupling picture. The large amount of $\ell = 2$ strength found at ∼5 MeV has been identified as large low-lying fragments of the neutron $0d_{3/2}$ strength. Assuming the same normalization factor as used for the $\nu 0d_{5/2}$ strength, the normalized $0d_{3/2}$ strength is $\sum GS = 1.68(13)$, less than half of the expected vacancy of an empty orbital ($\sum GS = 4$). The remaining $\nu 0d_{3/2}$ strength resides above $S_n = 5.230(13)$ MeV [18], a region not probed in the present work.

It is worth noting that while the present measurement is not directly sensitive to strength originating from either the $\nu 0d_{5/2}$

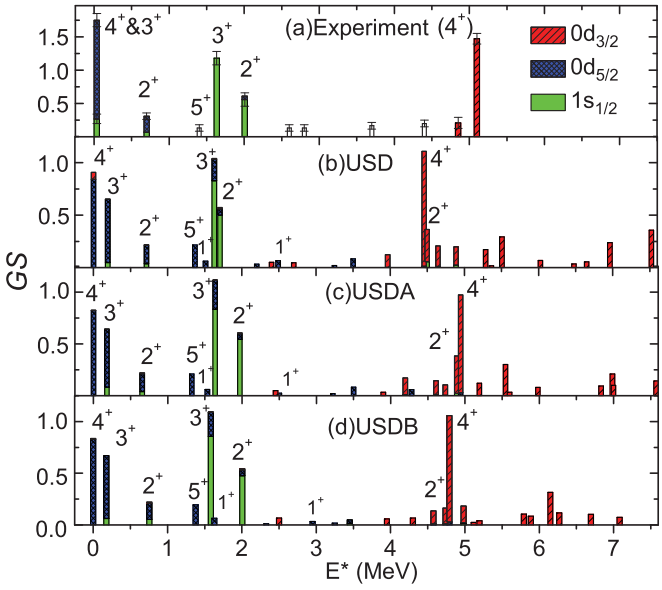

FIG. 4. Experimental (a) and calculated (b)–(d) $0d_{5/2}$ (blue cross-hatched bars), $1s_{1/2}$ (green bars), $0d_{3/2}$ (red slashed bars) single-neutron strengths as a function of excitation energy in ^{22}F using the (b) USD, (c) USDA, and (d) USDB interactions. The weaker strengths extracted assuming only $\ell = 2$ neutron transfer are represented by the white unfilled bars. States with calculated $S \leqslant 0.04$ were not included in the plots. Spin-parity labels are shown only for those levels which are relevant to the discussions in the text.

or $\nu 0d_{3/2}$ orbitals, very little mixing between the two strengths is expected due to their large energy separation ($\gtrsim$4 MeV). Of course, small amounts of fragmented strength may still be distributed between them, e.g., the weakly populated states residing between 2.2 and 4.6 MeV in excitation energy (Fig. 2 and Table I).

A. Shell model calculations

Single-neutron overlaps between levels in ^{22}F and the ^{21}F ground state have been calculated using the COSMO shell-model code [48] for the USD [5], USDA and USDB [12] *sd*-shell interactions. The resulting strengths are shown in Fig. 4(b)–4(d) together with the experimental values in Fig. 4(a), taken from Table I. Each calculation had a closed ^{16}O core and the valence particles were free to occupy all *sd* orbitals. A notable difference between the USDA/USDB interactions and the USD interaction is the proper reproduction of the oxygen drip line at $N = 16$ by the former two. The USD interaction incorrectly calculates the $N = 18$ ^{26}O ground state to be bound by $\sim$1 MeV.

The overall single-neutron strength distribution in ^{22}F is well reproduced by each of these *sd*-shell interactions. The agreement covers both the relative strengths between different states, as well as between different ℓ values within a single state. The $\ell = 2$ assumption for the weak strength observed between $\sim 2 < E^* < 4$ MeV also seems to be reasonable based on the calculated results.

Assignment of the newly found $\ell = 2$ strength around $E_x \approx 5$ MeV as corresponding to the $\nu 0d_{3/2}$ orbital is supported by the shell-model calculations. A tentative $J^\pi = (4^+)$ assignment has been made to the largest observed fragment at $E_x = 5.10(3)$ MeV based on a comparison with the calculated strength. However, both this level and the 4.85(5)-MeV level could be formed from a combination of $\nu 0d_{3/2}$ fragments as seen around $E^* \approx 5$ MeV, as suggested by the shell model calculations in Figs. 4(b) and 4(c). We assign a possible spin-parity range from $J^\pi = (1^+ - 4^+)$ for the 4.85(5) MeV level, with a slight favoring for the 2^+ based on the calculations.

Subtle discrepancies between the experimental data and the USD interaction are noticeable in Fig. 4. The spacing of the two levels comprising most of the $\nu 1s_{1/2}$ strength ($J^\pi = 2^+$ and 3^+) are compressed in the calculation, with the 2^+ state being too low in E^*. The calculated E^* of the lowest-lying significant $\nu 0d_{3/2}$ fragment ($J^\pi = 4^+$) is also $\sim$0.5 MeV lower than the data. The more recent USDA/USDB interactions seem to correct on these discrepancies reproducing the experimental $\ell = 0$ states, and have a better agreement with the measured energy of the lowest-lying $\nu 0d_{3/2}$ 4^+ level. On the latter point, the improved agreement of the USDA/USDB interactions with the data is rooted in the same mechanism responsible for their correct depiction of the $Z = 8$ drip line. Namely, an increase in the effective $\nu 0d_{3/2}$ orbital energy was found for the USDA/USDB interactions over that of the USD interaction.

B. $N = 14$ and 16 shell gaps

The size of the $N = 14$ shell gap in ^{22}F has been estimated to be 1.63(21) MeV from the difference in the weighted-centroid energies of the $\nu 0d_{5/2}$ [$E^* = 0.13(11)$ MeV] and $\nu 1s_{1/2}$ [$E^* = 1.76(18)$ MeV] strengths. An average E^* of 0.035 MeV was used for the g.s. (4^+) and 0.071-MeV (3^+) levels to determine the $\nu 0d_{5/2}$ centroid energy. Along with these, the 0.71-MeV (2^+) state was included in the centroid energy determination. An additional uncertainty of 100 keV is included on the $\nu 0d_{5/2}$ centroid energy to account for missing members of the multiplet (0^+, 1^+, and 5^+). If the upper limit on the strength of the previously observed 5^+ level at 1.4 MeV were to be included then the centroid energy would be 0.26(12) MeV. Only the two large $\ell = 0$ fragments were used in the $\nu 1s_{1/2}$ centroid determination and an additional uncertainty of 50 keV was added due to possible missed strength. The present value for the $N = 14$ gap size is in reasonable agreement with the neutron-rich oxygen isotopes which are known to have a subshell closure at $N = 14$ [17,27], but a little lower than than the value in ^{22,23}O [49,50]. However, it is comparably larger than the $N = 14$ gap in the C isotopes where a reduction of the shell gap has been observed [51,52].

The present data provide a lower limit on the $N = 16$ shell gap in ^{22}F of $\gtrsim$3 MeV. The difference in the weighted-centroid energies of the $\nu 1s_{1/2}$ [$E^* = 1.76(18)$ MeV] and $\nu 0d_{3/2}$ [$E^* \gtrsim 5$ MeV] strengths were used. Only a lower limit could be determined due to missed $\nu 0d_{3/2}$ strength at higher excitation energy above the S_n in ^{22}F. In other $N = 13$ nuclei, the same energy gap has been measured: ^{21}O = 3.98(10) MeV [27], and ^{23}Ne = 2.97(10) [47]. Similarly, the values for other neutron-rich oxygen isotopes are: ^{23}O = 4.00(2) MeV [28], ^{24}O = 4.95(16) MeV [31], and ^{25}O = 4.86(13) MeV [29]. As pointed out above, the location of the $\nu 0d_{3/2}$ strength in ^{22}F

TABLE II. Energy centroids, E^*_J and diagonal particle-hole TBMEs, $E^{\prime(p-h)}_J(0d_{5/2}{}^2)$ from the present data on ^{22}F, as well as particle-particle TBMEs, $E^{(p-p)}_J(0d_{5/2}{}^2)$, from the present data (^{22}F), particle-particle spectra of ^{18}F-^{18}O, and hole-hole spectra of ^{26}Al-^{26}Mg and ^{20}O. The $E^{(p-p)}_J(0d_{5/2}{}^2)$ determined from the calculated spectra of the USDA interaction [12] are also given for ^{18}F-^{18}O and ^{22}F. Uncertainties for the ^{22}F $E^{(p-p)}_J(0d_{5/2}{}^2)$ are discussed in text, while for the rest nuclei, they are estimated to be a few hundred keV.

		$E^{\prime(p-h)}_J(0d_{5/2}{}^2)$	$E^{(p-p)}_J(0d_{5/2}{}^2)$					
J	E^*_J	^{22}F	^{22}F	^{18}F-^{18}O [54,55]	^{26}Al-^{26}Mg [56,57]	^{20}O [17]	USDA ^{22}F	USDA ^{18}F-^{18}O
0[a]	9.25	9.95	−2.03	−2.77	−3.65	−2.74	−2.99	−3.37
1[a]	2.10	2.80	−3.70	−5.01	−2.92		−3.13	−3.32
2	1.02	1.72	−0.65	−1.06	−0.71	−1.37	−0.72	−0.92
3	0.07	0.77	−1.90	−1.69	−1.66		−1.89	−1.97
4	0.00	0.70	0.47	−0.36	0.81	0.53	0.15	−0.55
5	1.41	2.11	−3.31	−3.89	−3.56		−3.71	−3.90

[a]Not observed in the present measurement. See details in the text.

observed below S_n is better reproduced by the USDA and USDB interactions. With respect to the $N = 16$ shell gap, these two interactions predict $\gtrsim$3.2 MeV and $\gtrsim$3.1 MeV, as compared to the USD interaction with $\gtrsim$2.8 MeV.

C. Diagonal two-body matrix elements

Diagonal two-body matrix elements (TBMEs) of the effective nucleon-nucleon (NN) interaction, $E^{(p-p)}_J(j_1 j_2) = \langle j_1, j_2 J|V|j_1, j_2 J\rangle$, may be derived from the experimental data through measured $(2J+1)S$-weighted excitation energies and ground-state binding energies. Here, j_1, j_2, and J stand for the two interacting single-particle orbitals and the total angular momentum that they may couple to. In the present work, the low-lying structure of ^{22}F has been observed to be dominated by the coupling of single proton *particle* in a $0d_{5/2}$ orbital to a single-neutron *hole* in a $0d_{5/2}$ orbital, namely $j_1 = j_2 = 0d_{5/2}$ (Fig. 4 and Table I). This is consistent with the doubly-magic nature of ^{22}O acting as a robust core [18]. Therefore, the diagonal TBMEs $E^{(p-p)}_J(0d_{5/2}{}^2) = \langle 0d_{5/2}{}^2 J|V|0d_{5/2}{}^2 J\rangle$ may be extracted from the measured particle-hole matrix elements, $E^{\prime(p-h)}_J 0d_{5/2}{}^2$, in ^{22}F following conversion via the Pandya transformation [53]. The procedure used below follows that described in Ref. [7].

The excitation energy in ^{22}F where the $(0d_{5/2})^2$, $J = 0$–5 multiplet would appear degenerate in the absence of a residual interaction, and its energy would be

$$E_0(\pi 0d_{5/2}\nu 0d_{5/2}) = B[^{21}\mathrm{O}] + B[^{23}\mathrm{F}] - B[^{22}\mathrm{F}] - B[^{22}\mathrm{O}] = -0.70\,\mathrm{MeV}, \quad (2)$$

where $B[^A Z]$ are ground-state binding energies, and $B[^{21}\mathrm{O}]$ and $B[^{23}\mathrm{F}]$ are the $5/2^+$ neutron single-hole and proton single-particle ground states. The particle-hole TBME for a specified J value is then

$$E^{\prime(p-h)}_J\left(0d_{5/2}{}^2\right) = E^*_J - E_0(\pi 0d_{5/2}\nu 0d_{5/2}), \quad (3)$$

where E^*_J represent the centroids from the $(2J+1)S$-weighted excitation energies in ^{22}F (Table II). The E^*_J for $J = 2, 3, 4$, and 5 were determined using the spectroscopic information and energies given in Table I. The uncertainties in these centroids are estimated at around 150 keV. No levels needed to calculate the 0^+ and 1^+ centroids were directly identified in the present work. However, past work identified two 1^+ states at $E^* = 1.628$ MeV and 2.571 MeV and we took their average energy (2.10 MeV) to be E^*_1 [18]. The uncertainty in this centroid is taken to be ∼450 keV, the energy spanning the two 1^+ states. Calculations using the USDA interaction predict $E^*_1 = 1.93$ MeV, consistent with our estimate. The 0^+ state that we are interested in for the TBMEs is the isobaric analog of the ground state of ^{22}O [37] and should differ from it almost entirely by the Coulomb energy difference which is constant to better than 100 keV across a given isotopic chain in this region of nuclei. It has isospin of $T = 3$ (and all the other members of the multiplet have $T = 2$). The uncertainty in the 0^+ energy is estimated at ∼100 keV.

The E^*_J, $E^{(p-h)}_J(0d_{5/2}{}^2)$, and $E^{(p-p)}_J(0d_{5/2}{}^2)$ values determined in the present work are listed in the second to fourth columns of Table II. The uncertainty on the ^{22}F $E^{(p-p)}_J(0d_{5/2}{}^2)$ values has been estimated to be ∼200 keV by varying the E^*_J across their uncertainties. The ^{22}F TBMEs can be directly compared to those which have been extracted in previous studies of particle-particle states in ^{18}F ($T = 0$) and ^{18}O ($T = 1$) [54,55], hole-hole states in ^{26}Al ($T = 0$) and ^{26}Mg ($T = 1$) [56,57], and hole-hole states ^{20}O ($T = 1$) [17] (Table II in columns five through seven). Similarly, the $E^{(p-p)}_J(0d_{5/2}{}^2)$ obtained from the calculated spectra of the USDA interaction for ^{18}F-^{18}O and ^{22}F are also listed in Table II.

The average interaction energy between two $0d_{5/2}$ nucleons, $\overline{E} = \sum_J (2J+1)E^{(p-p)}_J(0d_{5/2}{}^2)/\sum_J(2J+1)$, is the monopole component of the two-body interaction used in discussing the evolution of single-particle states by [58], was calculated from the ^{22}F, ^{18}F-^{18}O, and ^{26}Al-^{26}Mg TBMEs. The results are presented in Table III along with the same monopole energy extracted in two complementary methods [59,60] using the ground-state energy differences in ^{23}F-^{17}F and ^{28}Si-^{22}O [37]. Specifically, the ground-state one-proton separation energy, S_p, of the odd $(5/2^+)$ proton in ^{23}F outside of the complete proton $0p_{1/2}$ and neutron $0d_{5/2}$ shells of ^{22}O is six times larger than the ground-state S_p of ^{17}F from the empty neutron $0d_{5/2}$ orbital of ^{16}O. Similarly, were ^{28}Si a good closed shell for both $0d_{5/2}$ neutrons and protons, a comparison of its binding energy with that of ^{22}O and ^{16}O

TABLE III. The monopole component of the $E_J^{(p-p)}(0d_{5/2}{}^2)$ two-body interaction, $\overline{E}$, extracted from various empirical sources. Additional details are given in the text. The uncertainties are estimated to be a few hundred keV.

Nuclei used	$\overline{E}$ (MeV)	Method
^{18}F-^{18}O	−2.2	$\overline{E}$ relative to binding of a n and p on ^{16}O
^{23}F-^{17}F	−2.1	proton separation energy with full and empty $\nu 0d_{5/2}^6$ shell
^{22}F	−1.7	$\overline{E}$ relative to binding of a neutron-hole and a proton on ^{22}O
^{28}Si-^{22}O	(−1.8)[a]	Binding of $\pi 0d_{5/2}^6$ with full $\nu 0d_{5/2}^6$ shell
^{26}Al-^{26}Mg	(−1.7)[a]	$\overline{E}$ relative to the n and p hole-energies on ^{28}Si

[a]Likely affected by the weak shell closures in ^{28}Si.

would yield the same information [59,60]. However, while the monopole energy extracted using ^{28}Si is in reasonable agreement with the others, it should be considered with caution due to the ample information that the $0d_{5/2}$ shell in ^{28}Si is far from closed, unlike the closure of the $0p$-shell in the oxygen isotopes [61].

The $\overline{E}$ in Table III show on average a decrease in the interaction strength as a function of A ($A = 19$ and 25 are assumed for rows 2 and 4, respectively). The decrease is understood as the size of the orbits involved are increasing while the interaction strength remains constant [7]. Therefore, an A dependence has been included in a number of effective shell-model calculations, for example the USD and USDA/B interactions each employ a $\propto A^{-0.3}$ scale [5,12]. However, suggestions have also been made for a mass-scaling based on changes in the nuclear surface area, $\propto A^{-2/3}$ [62], as well as a simple $\propto A^{-1}$. While the data in Table III are slightly improved with some A-dependent scaling, the uncertainties are too large to conclude whether A scaling is present, and what functional form it may have.

The sd-shell USDA interaction reproduces well the energies and strengths of a number of nuclei in the O-F region. Hence, it is not surprising that its calculated $E_J^{(p-p)}(0d_{5/2}{}^2)$ values agree with the experimental values on the order of a few hundred keV. No significant trend in the differences between the calculated TBMEs and the data was observed outside of the experimental uncertainties when going from ^{18}F-^{18}O, located at the line of stability, to the slightly more neutron-rich ^{22}F. This is perhaps not surprising as the $\nu 0d_{5/2}$ levels of interest are well bound in both cases by >7 MeV and $\sim$5 MeV below their respective S_n values [18,63]. The present work does not directly add to the previous discussions surrounding the observed weakening of the observed $0d_{5/2}$-$0d_{3/2}$ TBMEs relative to their calculated counterparts as a function of binding energy [9,10]. However, it should be noted that the extraction of the *same* TBMEs from various sets of data, including single-particle strength distributions as done here for the $E_J^{(p-p)}(0d_{5/2}{}^2)$ (Tables II and III), show variation on the order of hundreds of keV. Using this information as a basis for applying systematic uncertainties to TBMEs has put the uncertainties on the same order as the recently observed differences between data and theory ($\sim$300 keV) [9,10].

The deviations of the $J = 0$ and 1 TBMEs between experimental results, independent of any A dependence, are found to be larger than for the other J values. One contributor to this effect is the additional energy present from pairing correlations in TBMEs which have been extracted from particle-particle data versus those extracted from particle-hole data. The weakened $J = 0$ TBME from the particle-hole data in the ^{22}F relative to all other TBMEs, in particular from ^{18}F-^{18}O particle-particle spectra, supports this observation. However, it should be pointed out that low-J states, and the $J = 0, 1$ states in particular, are the most experimentally demanding to observe due to their relatively small cross sections and resulting increased uncertainties.

V. SUMMARY

Single-neutron overlaps between final states in ^{22}F and the ground state of ^{21}F have been determined from the measured cross sections of the (d, p) reaction at 10 MeV/u in inverse kinematics. Spectroscopic factors and strengths were extracted from a DWBA analysis and the strength distributions of the $\nu 0d_{5/2}$, $\nu 1s_{1/2}$, and $\nu 0d_{3/2}$ orbitals are well reproduced by shell-model calculations using the USDA and USDB interactions. Calculations using the USD interaction underestimate the observed large $0d_{3/2}$ strength by around 0.5 MeV, hence, reinforcing USDA/USDB interactions depiction of an increased $0d_{3/2}$ single-particle energy in order to correctly reproduce the $Z = 8$ drip line. Estimates of the size of the $N = 14$ shell gap and a lower limit of the $N = 16$ shell gap were deduced in ^{22}F from information on weighted centroids. An independent determination of the diagonal $(0d_{5/2})_J^2$ two-body matrix elements was also obtained from the data through use of the Pandya transformation. Along with an extracted monopole component, they were compared with previous determinations of the same matrix element based on various sets of particle-particle or hole-hole spectra, as well as ground state binding energies. Outside of the large variations for the $J = 0$ and $J = 1$ energies, likely related to pairing energies, an overall agreement between them, on the order of a few hundred keV, was found and was further improved when a mass dependence of the matrix elements was considered.

ACKNOWLEDGMENTS

The authors would like to acknowledge the hard work of the support and operations staff at ATLAS. This research used resources of Argonne National Laboratory's ATLAS facility, which is a Department of Energy Office of Science User Facility. This material is based upon work supported by the U.S. Department of Energy, Office of Science, Office of Nuclear Physics, under Contract No. DE-AC02-06CH11357 (ANL) and Grant No. DE-FG02-96ER40978 (LSU). This work was also supported in part by the National Science Foundation under Grant No. NSF-1713857 with the University of Notre Dame. J.C. acknowledges partial support by the FRIB-CSC Fellowship under Grant No. 201600090345.

[1] M. Mayer and J. Jensen, *Elementary Theory of Nuclear Shell Structure*, Structure of Matter Series (John Wiley & Sons, New York, 1955).

[2] M. G. Mayer, Phys. Rev. **78**, 22 (1950).

[3] D. Kurath, Phys. Rev. **80**, 98 (1950).

[4] I. Talmi, Phys. Rev. **82**, 101 (1951).

[5] B. A. Brown and B. H. Wildenthal, Annu. Rev. Nucl. Part. Sci. **38**, 29 (1988).

[6] E. K. Warburton and B. A. Brown, Phys. Rev. C **46**, 923 (1992).

[7] J. P. Schiffer and W. W. True, Rev. Mod. Phys. **48**, 191 (1976).

[8] B. A. Brown, Int. J. Mod. Phys. E **26**, 1740003 (2017).

[9] A. Lepailleur, K. Wimmer, A. Mutschler, O. Sorlin, J. C. Thomas, V. Bader, C. Bancroft, D. Barofsky, B. Bastin, T. Baugher, D. Bazin, V. Bildstein, C. Borcea, R. Borcea, B. A. Brown, L. Caceres, A. Gade, L. Gaudefroy, S. Grévy, G. F. Grinyer, H. Iwasaki, E. Khan, T. Kröll, C. Langer, A. Lemasson, O. Llidoo, J. Lloyd, E. Lunderberg, F. Negoita, F. de Oliveira Santos, G. Perdikakis, F. Recchia, T. Redpath, T. Roger, F. Rotaru, S. Saenz, M.-G. Saint-Laurent, D. Smalley, D. Sohler, M. Stanoiu, S. R. Stroberg, M. Vandebrouck, D. Weisshaar, and A. Westerberg, Phys. Rev. C **92**, 054309 (2015).

[10] M. Vandebrouck *et al.* (R3B collaboration), Phys. Rev. C **96**, 054305 (2017).

[11] D. Steppenbeck, A. Deacon, S. Freeman, R. Janssens, M. Carpenter, C. Hoffman, B. Kay, T. Lauritsen, C. Lister, D. O'Donnell, J. Ollier, D. Seweryniak, J. Smith, K.-M. Spohr, S. Tabor, V. Tripathi, P. Wady, and S. Zhu, Nucl. Phys. A **847**, 149 (2010).

[12] B. A. Brown and W. A. Richter, Phys. Rev. C **74**, 034315 (2006).

[13] I. Stefan, F. de Oliveira Santos, O. Sorlin, T. Davinson, M. Lewitowicz, G. Dumitru, J. C. Angélique, M. Angélique, E. Berthoumieux, C. Borcea, R. Borcea, A. Buta, J. M. Daugas, F. de Grancey, M. Fadil, S. Grévy, J. Kiener, A. Lefebvre-Schuhl, M. Lenhardt, J. Mrazek, F. Negoita, D. Pantelica, M. G. Pellegriti, L. Perrot, M. Ploszajczak, O. Roig, M. G. Saint Laurent, I. Ray, M. Stanoiu, C. Stodel, V. Tatischeff, and J. C. Thomas, Phys. Rev. C **90**, 014307 (2014).

[14] W. N. Catford, "What can we learn from transfer, and how is best to do it?" in *The Euroschool on Exotic Beams*, Vol. IV, edited by C. Scheidenberger and M. Pfützner (Springer, Berlin/Heidelberg, 2014), pp. 67–122.

[15] D. Santiago-Gonzalez, K. Auranen, M. L. Avila, A. D. Ayangeakaa, B. B. Back, S. Bottoni, M. P. Carpenter, J. Chen, C. M. Deibel, A. A. Hood, C. R. Hoffman, R. V. F. Janssens, C. L. Jiang, B. P. Kay, S. A. Kuvin, A. Lauer, J. P. Schiffer, J. Sethi, R. Talwar, I. Wiedenhöver, J. Winkelbauer, and S. Zhu, Phys. Rev. Lett. **120**, 122503 (2018).

[16] J. Chen, J. Lou, Y. Ye, Z. Li, D. Pang, C. Yuan, Y. Ge, Q. Li, H. Hua, D. Jiang, X. Yang, F. Xu, J. Pei, J. Li, W. Jiang, Y. Sun, H. Zang, Y. Zhang, N. Aoi, E. Ideguchi, H. Ong, J. Lee, J. Wu, H. Liu, C. Wen, Y. Ayyad, K. Hatanaka, D. Tran, T. Yamamoto, M. Tanaka, and T. Suzuki, Phys. Lett. B **781**, 412 (2018).

[17] C. R. Hoffman, B. B. Back, B. P. Kay, J. P. Schiffer, M. Alcorta, S. I. Baker, S. Bedoor, P. F. Bertone, J. A. Clark, C. M. Deibel, B. DiGiovine, S. J. Freeman, J. P. Greene, J. C. Lighthall, S. T. Marley, R. C. Pardo, K. E. Rehm, A. Rojas, D. Santiago-Gonzalez, D. K. Sharp, D. V. Shetty, J. S. Thomas, I. Wiedenhöver, and A. H. Wuosmaa, Phys. Rev. C **85**, 054318 (2012).

[18] M. Shamsuzzoha Basunia, Nuclear Data Sheets **127**, 69 (2015).

[19] F. J. Vaughn, R. A. Chalmers, L. F. Chase, and S. R. Salisbury, Phys. Rev. Lett. **15**, 555 (1965).

[20] N. M. Clarke, P. R. Hayes, M. B. Becha, K. I. Pearce, R. J. Griffiths, J. B. A. England, L. Zybert, C. N. Pinder, G. M. Field, and R. S. Mackintosh, Jour. Phys. G: Nucl. Phys. **14**, 1399 (1988).

[21] R. H. Stokes and P. G. Young, Phys. Rev. **178**, 1789 (1969).

[22] N. Orr, L. Fifield, W. Catford, and C. Woods, Nucl. Phys. A **491**, 457 (1989).

[23] L. Weissman, A. F. Lisetskiy, O. Arndt, U. Bergmann, B. A. Brown, J. Cederkall, I. Dillmann, O. Hallmann, L. Fraile, S. Franchoo, L. Gaudefroy, U. Köster, K.-L. Kratz, B. Pfeiffer, and O. Sorlin, J. Phys. G: Nucl. Part. Phys. **31**, 553 (2005).

[24] F. Hubert, J. P. Dufour, R. Del Moral, A. Fleury, D. Jean, M. S. Pravikoff, H. Delagrange, H. Geissel, K. H. Schmidt, and E. Hanelt, Zeitschrift für Physik A At. Nucl. **333**, 237 (1989).

[25] S. Lee, S. L. Tabor, A. Volya, A. Aguilar, P. C. Bender, T. A. Hinners, C. R. Hoffman, M. Perry, and V. Tripathi, Phys. Rev. C **76**, 034308 (2007).

[26] R. Firestone, Nucl. Data Sheets **127**, 1 (2015).

[27] B. Fernández-Domínguez, J. S. Thomas, W. N. Catford, F. Delaunay, S. M. Brown, N. A. Orr, M. Rejmund, M. Labiche, M. Chartier, N. L. Achouri, H. Al Falou, N. I. Ashwood, D. Beaumel, Y. Blumenfeld, B. A. Brown, R. Chapman, N. Curtis, C. Force, G. de France, S. Franchoo, J. Guillot, P. Haigh, F. Hammache, V. Lapoux, R. C. Lemmon, F. Maréchal, A. M. Moro, X. Mougeot, B. Mouginot, L. Nalpas, A. Navin, N. Patterson, B. Pietras, E. C. Pollacco, A. Leprince, A. Ramus, J. A. Scarpaci, N. de Séréville, I. Stephan, O. Sorlin, and G. L. Wilson, Phys. Rev. C **84**, 011301(R) (2011).

[28] Z. Elekes, Z. Dombrádi, N. Aoi, S. Bishop, Z. Fülöp, J. Gibelin, T. Gomi, Y. Hashimoto, N. Imai, N. Iwasa, H. Iwasaki, G. Kalinka, Y. Kondo, A. A. Korsheninnikov, K. Kurita, M. Kurokawa, N. Matsui, T. Motobayashi, T. Nakamura, T. Nakao, E. Y. Nikolskii, T. K. Ohnishi, T. Okumura, S. Ota, A. Perera, A. Saito, H. Sakurai, Y. Satou, D. Sohler, T. Sumikama, D. Suzuki, M. Suzuki, H. Takeda, S. Takeuchi, Y. Togano, and Y. Yanagisawa, Phys. Rev. Lett. **98**, 102502 (2007).

[29] C. R. Hoffman, T. Baumann, D. Bazin, J. Brown, G. Christian, P. A. DeYoung, J. E. Finck, N. Frank, J. Hinnefeld, R. Howes, P. Mears, E. Mosby, S. Mosby, J. Reith, B. Rizzo, W. F. Rogers, G. Peaslee, W. A. Peters, A. Schiller, M. J. Scott, S. L. Tabor, M. Thoennessen, P. J. Voss, and T. Williams, Phys. Rev. Lett. **100**, 152502 (2008).

[30] National Nuclear Data Center, http://www.nndc.bnl.gov/.

[31] C. Hoffman, T. Baumann, D. Bazin, J. Brown, G. Christian, D. Denby, P. DeYoung, J. Finck, N. Frank, J. Hinnefeld, S. Mosby, W. Peters, W. Rogers, A. Schiller, A. Spyrou, M. Scott, S. Tabor, M. Thoennessen, and P. Voss, Phys. Lett. B **672**, 17 (2009).

[32] C. R. Hoffman, B. P. Kay, and J. P. Schiffer, Phys. Rev. C **94**, 024330 (2016).

[33] G. Mairle, L. K. Pao, G. J. Wagner, K. T. Knöpfle, and H. Riedesel, Zeitschrift für Physik A At. Nucl. **301**, 157 (1981).

[34] B. Harss, R. C. Pardo, K. E. Rehm, F. Borasi, J. P. Greene, R. V. F. Janssens, C. L. Jiang, J. Nolen, M. Paul, J. P. Schiffer, R. E. Segel, J. Specht, T. F. Wang, P. Wilt, and B. Zabransky, Rev. Sci. Instrum. **71**, 380 (2000).

[35] A. Wuosmaa, J. Schiffer, B. Back, C. Lister, and K. Rehm, Nucl. Instrum. Methods Phys. Res. A **580**, 1290 (2007).

[36] J. Lighthall, B. Back, S. Baker, S. Freeman, H. Lee, B. Kay, S. Marley, K. Rehm, J. Rohrer, J. Schiffer, D. Shetty, A. Vann, J. Winkelbauer, and A. Wuosmaa, Nucl. Instrum. Methods Phys. Res. A **622**, 97 (2010).
[37] W. J. Huang, G. Audi, M. Wang, F. G. Kondev, S. Naimi, and X. Xu, Chin. Phys. C **41**, 030002 (2016).
[38] J. Chen, J. L. Lou, Y. L. Ye, Z. H. Li, Y. C. Ge, Q. T. Li, J. Li, W. Jiang, Y. L. Sun, H. L. Zang, N. Aoi, E. Ideguchi, H. J. Ong, Y. Ayyad, K. Hatanaka, D. T. Tran, T. Yamamoto, M. Tanaka, T. Suzuki, N. T. Tho, J. Rangel, A. M. Moro, D. Y. Pang, J. Lee, J. Wu, H. N. Liu, and C. Wen, Phys. Rev. C **93**, 034623 (2016).
[39] J. Chen, J. L. Lou, Y. L. Ye, J. Rangel, A. M. Moro, D. Y. Pang, Z. H. Li, Y. C. Ge, Q. T. Li, J. Li, W. Jiang, Y. L. Sun, H. L. Zang, Y. Zhang, N. Aoi, E. Ideguchi, H. J. Ong, J. Lee, J. Wu, H. N. Liu, C. Wen, Y. Ayyad, K. Hatanaka, T. D. Tran, T. Yamamoto, M. Tanaka, T. Suzuki, and T. T. Nguyen, Phys. Rev. C **94**, 064620 (2016).
[40] Y. Han, Y. Shi, and Q. Shen, Phys. Rev. C **74**, 044615 (2006).
[41] W. W. Daehnick, J. D. Childs, and Z. Vrcelj, Phys. Rev. C **21**, 2253 (1980).
[42] A. Koning and J. Delaroche, Nucl. Phys. A **713**, 231 (2003).
[43] R. Varner, W. Thompson, T. McAbee, E. Ludwig, and T. Clegg, Phys. Rep. **201**, 57 (1991).
[44] H. An and C. Cai, Phys. Rev. C **73**, 054605 (2006).
[45] M. H. Macfarlane and S. C. Pieper, Report No. ANL-76-11, Rev. 1, 1978 (unpublished).
[46] R. B. Wiringa, V. G. J. Stoks, and R. Schiavilla, Phys. Rev. C **51**, 38 (1995).
[47] H. Lutz, J. Wesolowski, L. Hansen, and S. Eccles, Nucl. Phys. A **95**, 591 (1967).
[48] A. Volya, COSMO code, http://www.volya.net.
[49] M. Stanoiu, F. Azaiez, Z. Dombrádi, O. Sorlin, B. A. Brown, M. Belleguic, D. Sohler, M. G. Saint Laurent, M. J. Lopez-Jimenez, Y. E. Penionzhkevich, G. Sletten, N. L. Achouri, J. C. Anglique, F. Becker, C. Borcea, C. Bourgeois, A. Bracco, J. M. Daugas, Z. Dlouhý, C. Donzaud, J. Duprat, Z. Fülöp, D. Guillemaud-Mueller, S. Grévy, F. Ibrahim, A. Kerek, A. Krasznahorkay, M. Lewitowicz, S. Leenhardt, S. Lukyanov, P. Mayet, S. Mandal, H. van der Marel, W. Mittig, J. Mrázek, F. Negoita, F. De Oliveira-Santos, Z. Podolyák, F. Pougheon, M. G. Porquet, P. Roussel-Chomaz, H. Savajols, Y. Sobolev, C. Stodel, J. Timár, and A. Yamamoto, Phys. Rev. C **69**, 034312 (2004).
[50] A. Schiller, N. Frank, T. Baumann, D. Bazin, B. A. Brown, J. Brown, P. A. DeYoung, J. E. Finck, A. Gade, J. Hinnefeld, R. Howes, J.-L. Lecouey, B. Luther, W. A. Peters, H. Scheit, M. Thoennessen, and J. A. Tostevin, Phys. Rev. Lett. **99**, 112501 (2007).
[51] M. Stanoiu, D. Sohler, O. Sorlin, F. Azaiez, Z. Dombrádi, B. A. Brown, M. Belleguic, C. Borcea, C. Bourgeois, Z. Dlouhy, Z. Elekes, Z. Fülöp, S. Grévy, D. Guillemaud-Mueller, F. Ibrahim, A. Kerek, A. Krasznahorkay, M. Lewitowicz, S. M. Lukyanov, S. Mandal, J. Mrázek, F. Negoita, Y.-E. Penionzhkevich, Z. Podolyák, P. Roussel-Chomaz, M. G. Saint-Laurent, H. Savajols, G. Sletten, J. Timár, C. Timis, and A. Yamamoto, Phys. Rev. C **78**, 034315 (2008).
[52] M. J. Strongman, A. Spyrou, C. R. Hoffman, T. Baumann, D. Bazin, J. Brown, P. A. DeYoung, J. E. Finck, N. Frank, S. Mosby, W. F. Rogers, G. F. Peaslee, W. A. Peters, A. Schiller, S. L. Tabor, and M. Thoennessen, Phys. Rev. C **80**, 021302(R) (2009).
[53] S. P. Pandya, Phys. Rev. **103**, 956 (1956).
[54] L. M. Polsky, C. H. Holbrow, and R. Middleton, Phys. Rev. **186**, 966 (1969).
[55] T. K. Li, D. Dehnhard, R. E. Brown, and P. J. Ellis, Phys. Rev. C **13**, 55 (1976).
[56] G. Wagner, G. Mairle, U. Schmidt-Rohr, and P. Turek, Nucl. Phys. A **125**, 80 (1969).
[57] P. Endt and C. van der Leun, Nucl. Phys. A **214**, 1 (1973).
[58] T. Otsuka, T. Suzuki, J. D. Holt, A. Schwenk, and Y. Akaishi, Phys. Rev. Lett. **105**, 032501 (2010).
[59] M. Moinester, J. P. Schiffer, and W. P. Alford, Phys. Rev. **179**, 984 (1969).
[60] J. French, in *Nuclear Structure*, edited by A. Hosssin, H. Ar-Rashid, and M. Islam (Wiley-Interscience, New York, 1967).
[61] M. S. Basunia, Nucl. Data Sheets **114**, 1189 (2013).
[62] O. Sorlin and M.-G. Porquet, Prog. Part. Nucl. Phys. **61**, 602 (2008).
[63] D. Tilley, H. Weller, C. Cheves, and R. Chasteler, Nucl. Phys. A **595**, 1 (1995).